Identification and validation of biomarkers related to mitophagy in chronic obstructive pulmonary disease

JIE CHEN[1,2], XIAOFENG ZHANG[3] and GENGYUN SUN[1]

[1]Department of Respiratory and Critical Care Medicine, The First Affiliated Hospital of Anhui Medical University, Hefei, Anhui 230022, P.R. China; [2]Department of Respiratory and Critical Care Medicine, The Third Affiliated Hospital of Anhui Medical University (The First People's Hospital of Hefei), Hefei, Anhui 230061, P.R. China; [3]Department of General Medicine, The Second Affiliated Hospital of Anhui Medical University, Hefei, Anhui 230601, P.R. China

Received June 27, 2024; Accepted September 9, 2024

DOI: 10.3892/mmr.2025.13458

Abstract. Mitophagy plays significant roles in chronic obstructive pulmonary disease (COPD). The present study aimed to screen and validate mitophagy-related genes in COPD by using bioinformatic analysis and experimental validation. The original data were downloaded from Gene Expression Omnibus datasets and 29 mitophagy-related genes sets were acquired from the Molecular Signatures Database. The differentially expressed mitophagy-related genes (DEMRGs) were screened using the Wilcoxon test. Gene Ontology and Kyoto Encyclopedia of Genes and Genomes enrichment analysis were conducted for the identification of DEMRGs. In addition, clustering analysis was used to assess the differential expression characteristics of DEMRGs in patients with COPD. Least absolute shrinkage and selection operator (LASSO) regression analysis was performed to identify signature genes with COPD diagnostic significance; these genes were validated using the test dataset. In addition, the degree of infiltration of 28 immune cells in COPD and control samples was assessed. Finally, cigarette smoke extract (CSE)-treated bronchial epithelial cells were employed to verify the role of signature genes in regulating mitophagy *in vitro* using molecular biology approaches. A total of 14 DEMRGs were identified, which were mainly involved in mitophagy-related processes and pathways. Clustering analysis indicated the expression levels of 14 DEMRGs except for microtubule-associated protein 1 light chain-3β, which was significantly different. Moreover, combination with LASSO, receiver operating characteristic curve and the validation dataset resulted in the identification of the mitochondrial transcription termination factor 3 (MTERF3). The infiltrating abundance of the majority of the immune cells was higher in COPD samples than that noted in the control samples; MTERF3 demonstrated the optimal correlation with macrophages, myeloid-derived suppressor cells, regulatory T cells and activated cluster of differentiation 8 T cells. Further analysis revealed that MTERF3 expression was increased in CSE-treated 16HBE cells and knockdown of MTERF3 expression promoted mitophagy. These findings provide novel insights into the role of mitophagy in COPD and identify novel targets for COPD diagnosis and treatment.

Correspondence to: Dr Gengyun Sun, Department of Respiratory and Critical Care Medicine, The First Affiliated Hospital of Anhui Medical University, 218 Jixi Road, Shushan, Hefei, Anhui 230022, P.R. China
E-mail: gengyunSun0320@126.com

Key words: mitophagy, mitophagy-related genes, chronic obstructive pulmonary disease, MTERF3, bioinformatics analysis

Introduction

Chronic obstructive pulmonary disease (COPD), a common chronic respiratory lung ailment, is characterized by long-term airflow limitation that is not fully reversible. It is estimated that COPD will become the third leading cause of mortality by 2030 in the world (1). A total of 212.3 million patients with COPD have been reported in 2019 worldwide; this is estimated to increase to 600 million prevalent cases of COPD by 2050 worldwide (2,3). It is widely accepted that persistent exposure to cigarette smoke (CS) is by far the primary etiological factor for COPD and has been documented in >80% of COPD cases (4). As a serious health burden, COPD has an important impact on the quality of life of patients, and causes a huge socioeconomic and medical burden (5). Therefore, it is imperative to identify COPD biomarkers and elucidate the molecular mechanisms of pathogenesis involved in COPD.

Accumulated evidence indicates that multiple biological functions are implicated in the pathogenesis of COPD (6-8). Among them, autophagy exerts a crucial effect on the development of COPD (9). Autophagy is a highly conserved homeostatic process, during which autophagosomes devour and degrade damaged or aged organelles for further processing and recycling to maintain cellular homeostasis (10). Notably, autophagy eliminates the damaged mitochondria, a process known as mitophagy, which is the main part of the mitochondrial quality control system (11). Dysregulation of mitophagy contributes to the development of diverse lung disorders, including asthma, acute lung injury, bronchopulmonary dysplasia and COPD (12). Substantial evidence suggests that CS impairs mitophagy, resulting in the accumulation of

damaged mitochondria (13,14). By regulating mitophagy in cigarette smoke extract (CSE)-induced airway epithelial cells, MAPK15-Unc-51-like kinase signaling participates in the development of COPD (15). Nevertheless, the genes related to mitophagy in COPD have not been fully clarified and further studies are required for their identification. The exploration of the potential mitophagy-related genes during COPD development will provide the possibility of identifying potential biomarkers for the treatment of this condition.

In the present study, the mitophagy-associated differentially expressed genes (DEGs) were analyzed in the Gene Set Enrichment (GSE) 76925 dataset in COPD and control samples. The expression patterns of these DEGs were analyzed by cluster analysis. Subsequently, Gene Ontology (GO) and Kyoto Encyclopedia of Genes and Genomes (KEGG) enrichment analyses were performed for the identifications of DEGs and their biological functions and interaction networks were assessed. In addition, least absolute shrinkage and selection operator (LASSO) regression analysis was used to screen signature genes and analyze their relationship with immune cells. Finally, biological experiments were conducted to investigate the involvement of signature genes in the progression of COPD.

Materials and methods

Acquisition of datasets and mitophagy-related genes. The COPD datasets were downloaded from the Gene Expression Omnibus (GEO) datasets (http://www.ncbi.nlm.nih.gov/geo/) on December 5, 2023. The GSE76925 dataset which included 111 COPD samples and 40 control samples was downloaded from the GPL10558 platform and was used as the training set. In addition, a study of 18 patients with COPD and 36 control samples (GSE8545) downloaded from the GPL570 platform was selected as the validation set. The 'limma' R package (https://bioconductor.org/packages/release/bioc/html/limma.html) was employed to pre-process the raw microarray data for quality control. A total of 29 mitophagy-related genes sets (REACTOME_MITOPHAGY) were downloaded from the Molecular Signatures Database (MSigDB; https://www.gsea-msigdb.org/gsea/index.jsp).

Identification of differentially expressed mitophagy-related genes (DEMRGs). The DEMRGs identified in COPD and control samples were analyzed with the application of the Wilcoxon test. Plot box plots were made using the 'ggpubr' package (https://rpkgs.datanovia.com/ggpubr/).

GO and KEGG enrichment analysis. The GO and KEGG enrichment analyses were used to investigate the biological functions and signaling pathways for DEMRGs using 'ClusterProfiler' R package (https://yulab-smu.top/biomedical-knowledge-mining-book/). The results are visualized using the 'ggplot2' R package (https://ggplot2.tidyverse.org/).

Clustering and differential analyses. To analyze the differential expression characteristics of DEMRGs in patients with COPD, 'ConsensusClusterPlus' (https://www.bioconductor.org/packages/release/bioc/html/ConsensusClusterPlus.html) was used in the R package to perform hierarchical clustering according to the expression of DEMRGs. The parameter was set to 50 replicates (rep=50) with a resampling rate of 80% (pItem=0.8). The DEGs between clusters were analyzed by the 'limma' R package, using |log2FC| >1 and the adjusted P<0.05 was used as cutoff value. The Volcano plot of DEGs was generated using the 'ggrepel' package (https://ggrepel.slowkow.com/).

Screening for signature genes using LASSO regression analysis. LASSO regression analysis was conducted to screen genes with COPD diagnostic significance with the application of 'glmnet' R package (https://glmnet.stanford.edu/). The genes and their coefficients were determined by the optimal penalty parameter λ with a minimum 10-fold cross validation. Receiver operating characteristic (ROC) curve was employed to calculate the area under the curve (AUC) to accurately evaluate the validity of the signature genes as diagnostic markers. ROC curves were obtained using the R package 'pROC' (https://xrobin.github.io/pROC/).

Validation of the signature genes in the test set. The diagnostic performance was validated in validation sets (GSE8545) by calculating the AUC of the ROC curve. The ROC curves were plotted by means of the R software package 'pROC'.

Analysis of immune infiltration. The immune cell infiltration in the microenvironment, involving 28 immune cells, was analyzed by single-sample gene set enrichment analysis to obtain a score file representing the immune cell composition in each individual sample in the GSE76925 dataset. The immune cell scores of the COPD and control groups were statistically analyzed by the t-test. The results were visually represented by box plots. The association between signature genes and immune cells was analyzed with the application of the correlation test function in the R software (v.4.3.3; https://cran.r-project.org/). Subsequently, the results were visualized with the 'ggplot' R package. A correlation analysis was used to measure the relationship between the dysregulated immune cells and a signature gene, which was presented graphically.

Culture of 16HBE cells. The normal human bronchial epithelial cell line 16HBE was accessed from Procell Life Science & Technology Co., Ltd. The cells were nurtured in a mixture of RPMI-1640 medium (HyClone; Cytiva) containing 10% fetal bovine serum (HyClone; Cytiva), 100 U/ml penicillin and 0.1 mg/ml streptomycin (Beyotime Institute of Biotechnology) in an incubator at 37˚C in the presence of 5% CO_2.

Preparation of CSE and treatment. CSE was prepared as previously reported (16). The smoke of 2 3R4F reference cigarettes was bubbled through 10 ml RPMI-1640 medium. The CSE solution was titrated to pH 7.4 and sterilized by filtration through a 0.22-μm pore filter, which was regarded as 100% concentration of CSE. The solution was diluted to the required concentrations (0.5, 1, 2 and 4%) with RPMI-1640 medium to treat 16HBE cells for 24 h; the treatment aimed to simulate the lung cell destruction condition observed in COPD.

Cell viability assay. 16HBE cells were replanted in 96-well plates ($2x10^4$ cells/well). The following day, the cells were

cultured in fresh medium containing different concentrations of CSE (0.5, 1, 2 and 4%) for an additional 24 h. Subsequently, 10 μl Cell Counting Kit-8 (CCK-8) working liquid (cat. no. C0037; Beyotime Institute of Biotechnology) was mixed with each well and the samples were incubated for 2 h. The absorbance values at 450 nm were detected with a microplate reader (Bio-Rad Laboratories, Inc.).

Gene interference. Experiments with knockdown of expression of mitochondrial transcription termination factor 3 (MTERF3) were performed. Specifically, 16HBE cells were transfected with small interfering RNA (siRNA) targeting MTERF3 and the sequences were as follows: siRNA-MTERF3-1 (50 nM), sense, 5'-UGGAUUUGUCCA AGAUAGAAAAA-3', anti-sense, 5'-UUUUUCUAUCUUGGA CAAAUCCA-3'; siRNA-MTERF3-2 (50 nM), sense, 5'-AGG CUGUUUAAGGUCAAAGAAAG-3', anti-sense, 5'-CUU UCUUUGACCUUAAACAGCCU-3') or 50 nM scrambled negative control (siRNA-NC, sense, 5'-ACCACAAGAUGA AGAGCACCAAU-3', anti-sense, 5'-AUUGGUGCUCUUCAU CUUGUGGU-3') customized by Shanghai GeneChem Co., Ltd. The cells were transfected using Lipofectamine™ 3000 (Invitrogen; Thermo Fisher Scientific, Inc.) for 48 h at 37˚C following the operating instructions. The cells were cultured for 48 h at 37˚C following transfection and immunoblotting was adopted for the detection of the transfection efficiency.

Flow cytometric analysis. The induction of apoptosis of 16HBE cells was tested by using an Annexin V-fluorescein isothiocyanate (FITC)/propidium iodide (PI) Kit (cat. no. C1062L; Beyotime Institute of Biotechnology). 16HBE cells were seeded in a 6-well plate at a density of $1x10^5$/well. Following transfection and treatment with CSE, 16HBE cells were resuspended in binding buffer and stained with Annexin V-FITC and PI for 15 min in dark at 37˚C. The cells were quantified with flow cytometry (BD FACSCalibur; BD Biosciences). A total of 10,000 events were collected per sample and the apoptotic rate of the cells was analyzed using FlowJo 10.8 software (FlowJo; BD Biosciences).

Analysis of mitochondrial reactive oxygen species (mitoROS). The generation of mitoROS was assessed with the application of Mito SOX Red (cat. no. M36008; Invitrogen; Thermo Fisher Scientific, Inc.) assay. Specifically, 16HBE cells were seeded in 96 well plates ($5x10^4$ cells/ml). Following the indicated treatment, the cells were treated with 5 mM Mito SOX Red probe for 15 min at 37˚C. Subsequently, the cells were incubated with PBS and the fluorescence images were acquired using a fluorescence microscope (Olympus Corporation).

Assessment of oxidative stress markers. The levels of malonaldehyde (MDA; cat. no. A003-4-1) and superoxide dismutase (SOD; cat. no. A001-3-2) in the supernatant of cultured 16HBE cells were detected using the commercially available kits (Nianjing Jiancheng Bioengineering Institute). The absorbance value of the samples, at 530 nm for MDA and 450 nm for SOD, was detected using a microplate reader (Bio-Rad Laboratories, Inc.).

Detection of mitochondrial membrane potential (MMP). MMP was evaluated using the 5,5',6,6'-tetrachloro1,1',3,3'-tetramethylbenzimidazolylcarbocyanine iodide (JC-1) dye (cat. no. C2005; Beyotime Institute of Biotechnology). Following the indicated treatment, 16HBE cells were stained at 37˚C for 20 min with the JC-1 dye. Fluorescence images were obtained using a fluorescence microscope (Olympus Corporation). The red fluorescence represents the JC-1 aggregates, while the green fluorescence represents JC-1 monomers.

Immunoblotting. The cells were lysed with radioimmunoprecipitation assay buffer (Beyotime Institute of Biotechnology) to extract the total proteins. The total protein concentration was assessed with the application of the Bradford assay. Each quantity of boiled protein (40 μg) was added to 10% sodium dodecyl sulfate-polyacrylamide gel electrophoresis (SDS-PAGE) for separation; the proteins were subsequently transferred to the nitrocellulose films. Following 1 h blocking with 5% bovine serum albumin (Beyotime Institute of Biotechnology) at room temperature, these membranes were incubated with primary antibodies overnight at 4˚C. Subsequently, an anti-rabbit IgG HRP-linked secondary antibody (1:10,000; cat. no. 7074P2; Cell Signaling Technology, Inc.) was incubated with the transfer membranes. The detection was performed using the enhanced chemiluminescence (MilliporeSigma). GAPDH acted as a reference gene. The intensities of the proteins were assessed quantitatively using ImageJ Software (version 1.8.0; National Institutes of Health). The primary antibodies used were the following: Anti-MTERF3 (1:1,000; cat. no. ab230232) and anti-putative kinase 1 (PINK1; 1:1,000; cat. no. ab216144) antibodies were acquired from Abcam. Anti-B cell lymphoma-2 (Bcl-2; 1:1,000; cat. no. 3498T), anti-Bcl-2-associated X protein (Bax; 1:1,000; cat. no. 2772T), anti-cleaved casapse3 (1:1,000; cat. no. 9664T), anti-caspase3 (1:1,000; cat. no. 14220T), anti-LC3II/LC3I (1:1,000; cat. no. 12741T), anti-Beclin-1 (1:1,000; cat. no. 3495T), anti-p62 (1:1,000; cat. no. 5114T), anti-Parkin (1:1,000; cat. no. 2132S), anti-COX IV (1:1,000; cat. no. 4850T) and anti-GAPDH (1:1,000; cat. no. 2118T) antibodies were provided by Cell Signaling Technology, Inc.

Statistical analysis. The statistical analysis was performed using R software (v.4.3.3). Wilcoxon rank-sum test or unpaired Student's t-test was used to compare the significance differences between the two groups of samples. Adjusted $P<0.05$ was used as a threshold for significant difference. Results are shown as the mean ± standard deviation from three independent experiments. GraphPad 8.0 software (GraphPad; Dotmatics) was used for statistical analysis. The different groups were compared by one-way analysis of variance with post-hoc Tukey's analysis. $P<0.05$ was considered to indicate a statistically significant difference.

Results

Identification and functional enrichment analysis of DEMRGs. Dysregulation of mitophagy is involved in the development of COPD (17,18). To determine the mitophagy-related core gene profiles of patients with COPD, the collated datasets were downloaded from the GEO database. The information included in the study was listed in Table I. The GSE76925 dataset (COPD, 111; control, 40) was used to screen the DEGs.

Table I. Characteristics of the datasets used in the present study.

Dataset	Platform	Samples	Total	Normal	COPD
GSE76925	GPL10558	Lung tissue	141	40	111
GSE8545	GPL570	Airway epithelial cells	54	36	18

COPD, chronic obstructive pulmonary disease.

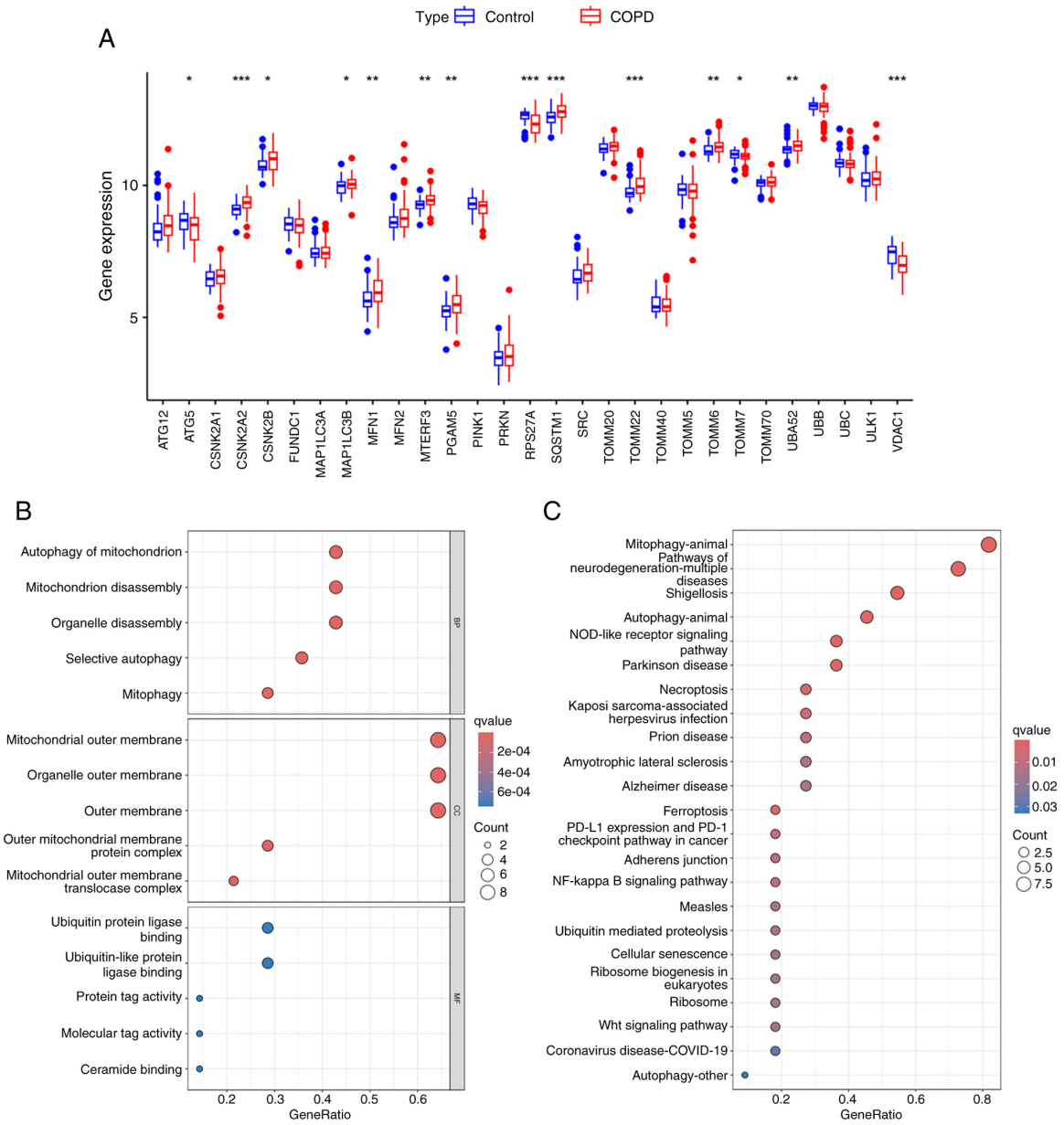

Figure 1. Identification and functional enrichment analysis of DEMRGs. (A) Plot box plots indicated the DEMRGs between COPD and control samples in the GSE76925 dataset (COPD, 111; control, 40). *P<0.05, **P<0.01 and ***P<0.001. (B) GO enrichment analysis of DEMRGs, including BP, CC and MF. (C) KEGG enrichment analysis of DEMRGs. The size of dots indicates the gene number and the shade of the color indicates the scale of -log10 (P-value). DEMRGs, differentially expressed mitophagy-related genes; COPD, chronic obstructive pulmonary disease; GO, Gene Ontology; BP, biological processes; CC, cellular components; MF, molecular functions; KEGG, Kyoto Encyclopedia of Genes and Genomes.

A total of 29 mitophagy-related genes were obtained from the MSigDB database. The expression levels of mitophagy-related genes in the 111 COPD and 40 control samples were analyzed. As displayed in Fig. 1A, among the 29 mitophagy-related genes, 14 genes demonstrated significant differences in their expression levels between the COPD and control samples (P<0.05); these were defined as DEMRGs. Subsequent GO analysis suggested that these DEMRGs were mainly involved

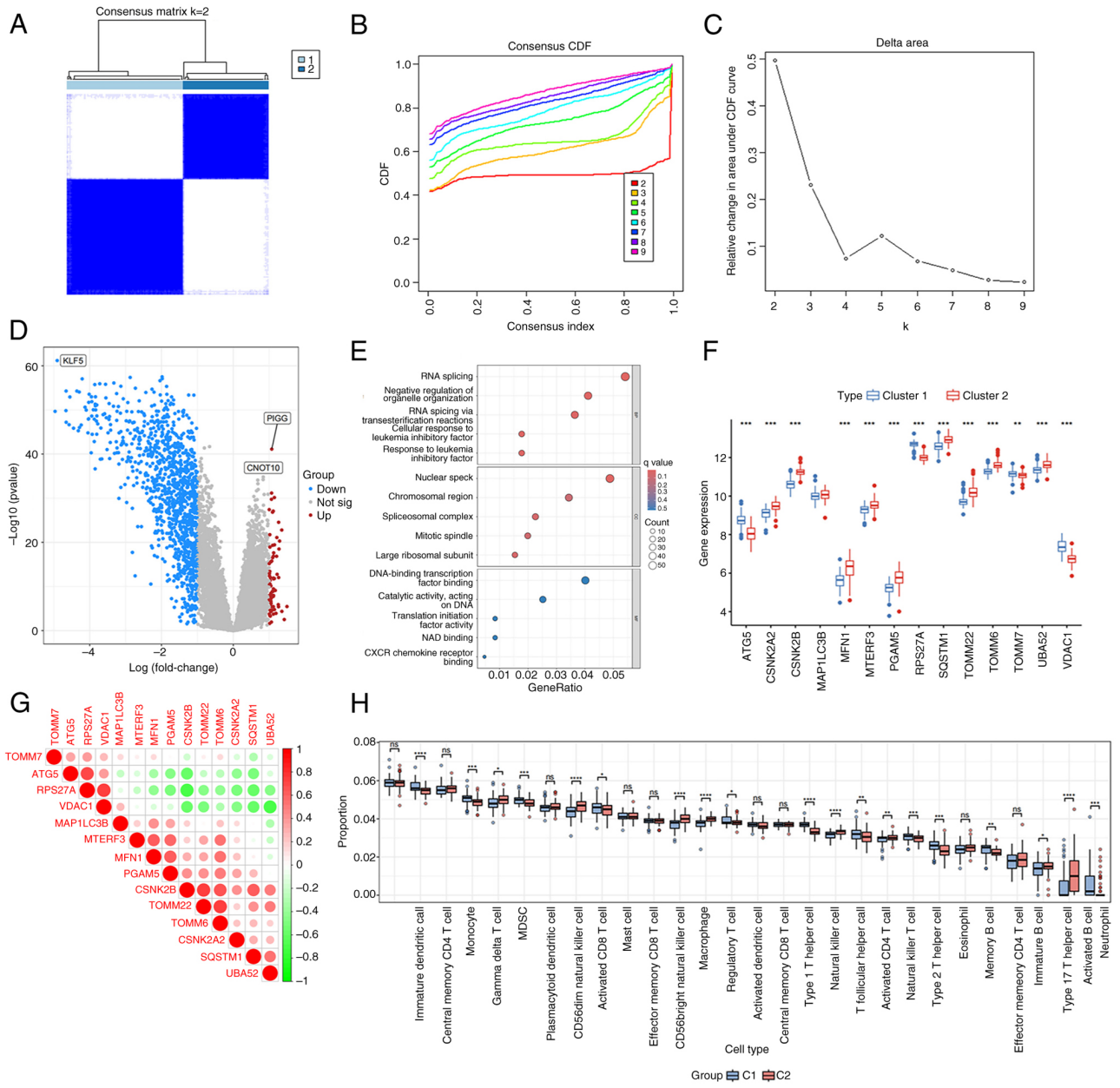

Figure 2. The expression pattern of DEMRGs. (A-C) Hierarchical cluster. (D) Volcano plot of 1,207 DEGs including 14 DEMRGs. The red and blue dots represent the upregulated and downregulated genes, respectively. (E) GO enrichment analysis of DEGs, including BP, CC and MF. (F) Plot box plots indicated the expression levels of DEMRGs between cluster 1 and 2. (G) Correlation analysis of 14 DEMRGs. (H) The proportion of 28 types of immune cells was analyzed in cluster 1 and 2. *P<0.05, **P<0.01, ***P<0.001 and ****P<0.0001. DEMRGs, differentially expressed mitophagy-related genes; DEGs, differentially expressed genes; GO, Gene Ontology; BP, biological processes; CC, cellular components; MF, molecular functions; ns, not significant.

in the biological processes of mitophagy, mitochondrial breakdown and selective autophagy (Fig. 1B). In addition, the results of the KEGG analysis, which indicated that DEMRGs were mainly enriched in mitophagy, the NOD receptor and the NF-κB signaling pathways were identified (Fig. 1C).

The expression pattern of DEMRGs. To explore the expression levels of DEMRGs in patients with COPD, hierarchical clustering analysis was performed in 111 COPD and 40 control samples according to the expression levels of these DEMRGs. All samples were divided into two groups (cluster1, n=87; cluster2, n=64; Fig. 2A-C). The DEGs between cluster 1 and 2 were analyzed and 1,207 DEGs were screened, of which 73 genes were upregulated and 1,134 genes were downregulated (Fig. 2D). These DEGs were mainly involved in biological processes, such as transcription and translation (Fig. 2E). In addition, the expression levels of these DEMRGs between cluster 1 and 2 were also explored. The results indicated that except for microtubule-associated protein 1 light chain-3β (MAP1LC3B), the expression levels of other genes were significantly different (Fig. 2F). To assess the correlation of the expression levels of DEMRGs, correlation analysis was conducted. As depicted in Fig. 2G, the expression of ribosomal protein S27A was positively correlated with the expression of voltage-dependent anion channel 1 (VDAC1), whereas it was negatively correlated with the expression levels of other genes. Moreover, strong interactions were noted between mitofusin-1 and phosphoglycerate mutase family member 5 (PGAM5) as

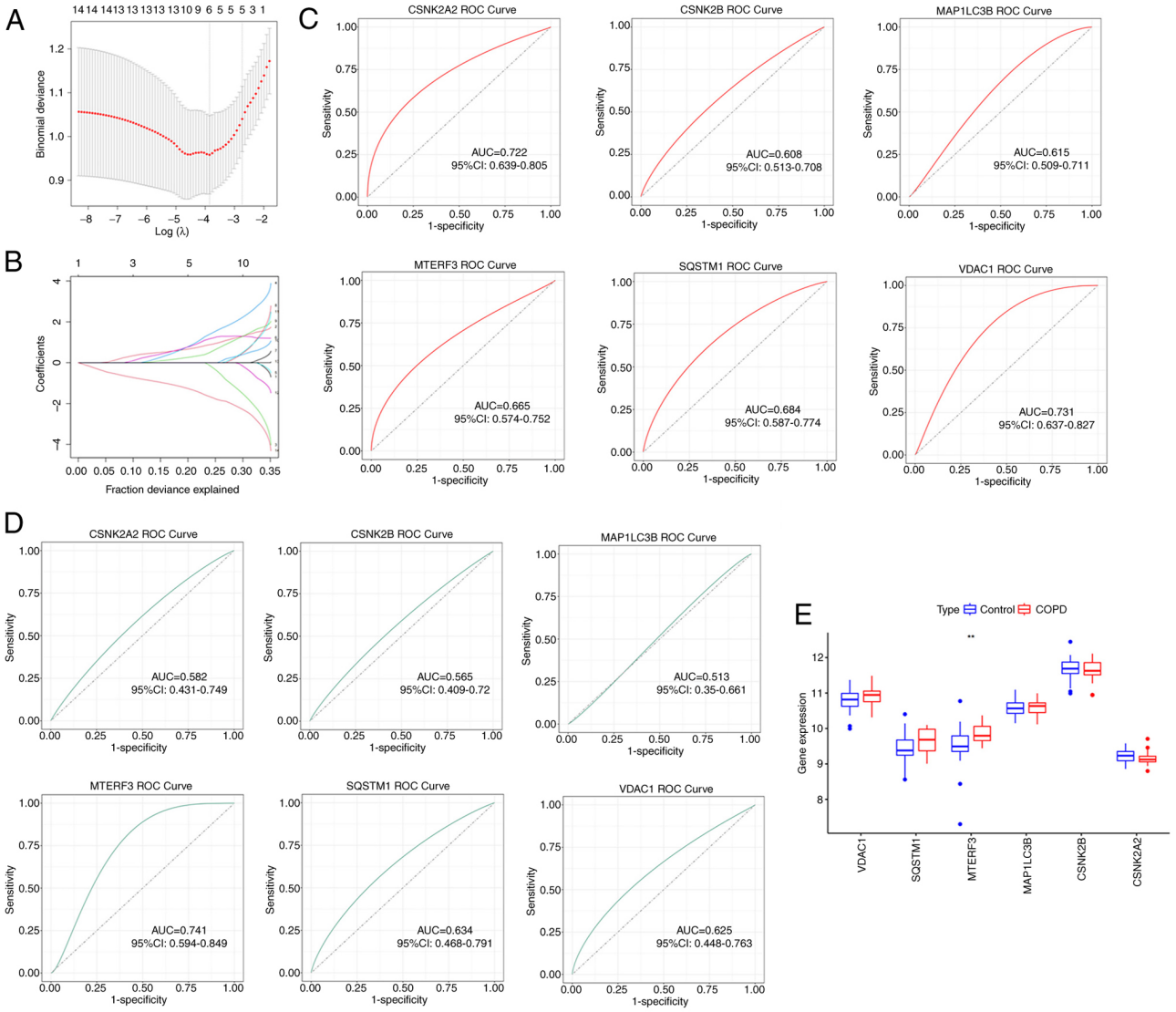

Figure 3. Selection and validation of COPD signature genes. (A) The plot of COPD signature genes was examined using LASSO regression analysis. (B) Lasso coefficients of LASSO regression screening genes. (C) The AUC values of the ROC curves for the 6 signature genes in GSE76925 dataset. (D) The AUC values of the ROC curves for the 6 signature genes in the GSE8545 dataset. (E) Plot box plots indicated the expression levels of 6 signature genes in COPD and control samples in the GSE8545 dataset. **P<0.01. COPD, chronic obstructive pulmonary disease; LASSO, least absolute shrinkage and selection operator; AUC, area under the curve; ROC, receiver operating characteristic.

well as with translocase of outer mitochondrial membrane 22 and TOMM6. Analysis of immune infiltration between cluster 1 and 2 is shown in Fig. 2H.

Selection and validation of COPD signature genes. To screen signature genes with COPD diagnostic significance, LASSO regression analysis was used in the present study. As shown in Fig. 3A and B, the optimal performance was achieved when 6 genes (CSNK2A2, CSNK2B, MAP1LC3B, MTERF3, SQSTM1 and VDAC1) were included in the LASSO regression analysis. Therefore, these 6 genes were identified as diagnostic markers for COPD. Subsequently, ROC curve was employed to calculate the AUC to accurately evaluate the validity of the signature genes as diagnostic markers. In the GSE76925 dataset, the AUC values of the ROC curves for the 6 signature genes are demonstrated in Fig. 3C. It was noted that CSNK2A2 (AUC: 0.722), MTERF3 (AUC: 0.665), SQSTM1 (AUC: 0.684) and VDAC1 (AUC: 0.731) exhibited the highest AUC values, suggesting that these 4 genes exhibited an optimal diagnostic value for distinguishing patients with COPD from control subjects. Subsequently, the 6 signature genes were validated in COPD using the GSE8545 dataset. As displayed in Fig. 3D, the AUC value of MTERF3 (AUC: 0.741) was the highest than that of other genes. In addition, only MTERF3 expression was significantly different between COPD and control samples (Fig. 3E). Therefore, the molecular mechanism of MTERF3 in COPD was further explored in subsequent experiments.

Immune cell infiltration in COPD and control samples. An increasing number of immune cell types have been associated with risk of COPD and prognosis of affected individuals (19,20). The degree of the infiltration of 28 immune cells in COPD and control samples was analyzed. As displayed in Fig. 4A, the infiltrating abundance of the majority of immune cells was higher in COPD samples than that observed in control samples. As revealed in Fig. 4B, immature

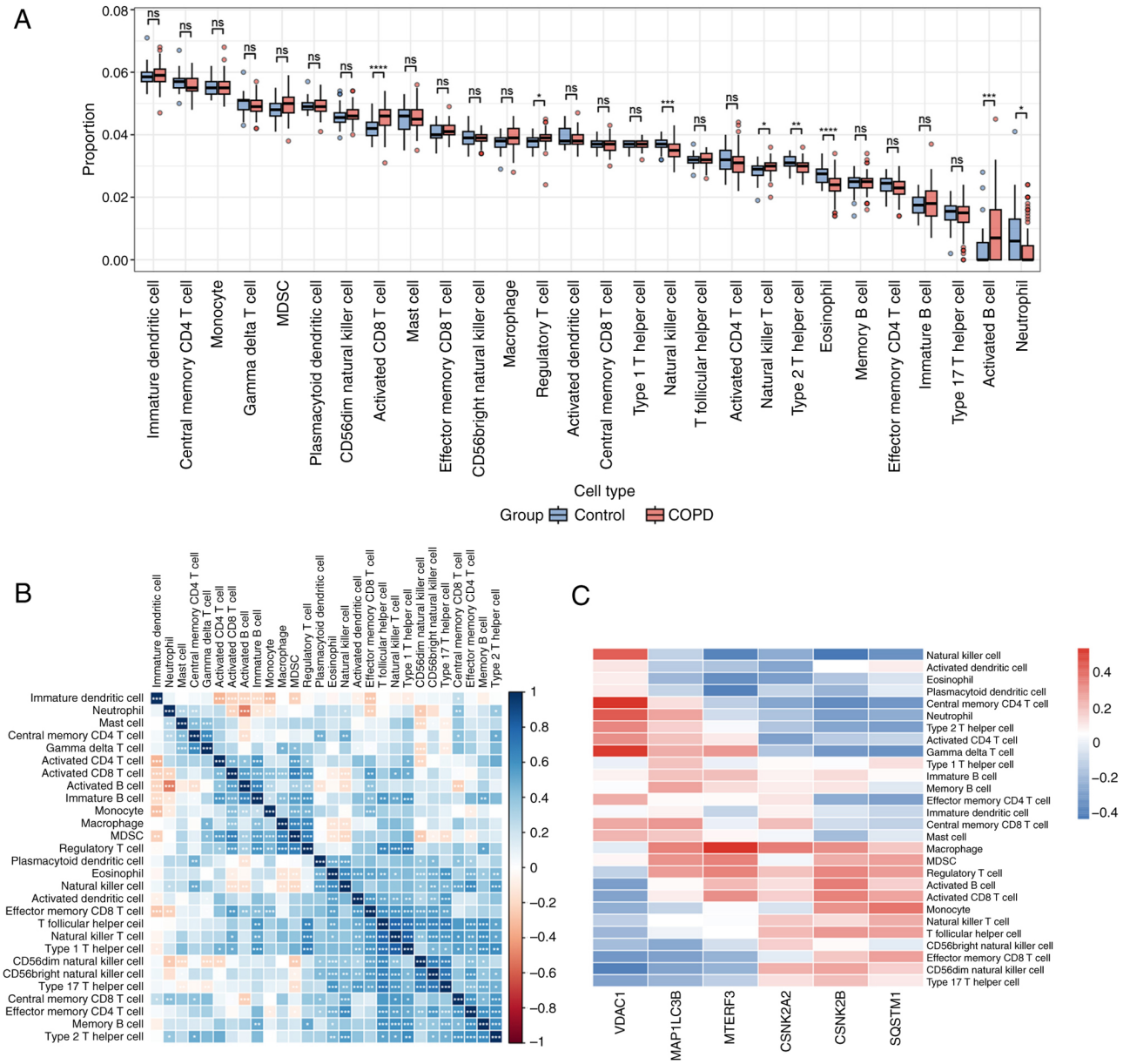

Figure 4. Immune cell infiltration in COPD and control samples. (A) Plot box plots indicated the degree of infiltration of 28 immune cells in COPD and control samples in the GSE76925 dataset. (B) Correlation analysis of the 28 immune cells. *P<0.05, **P<0.01, ***P<0.001 and ****P<0.0001. (C) Heatmap indicated the correlation between the expression of the six signature genes and the 28 types of immune cells. COPD, chronic obstructive pulmonary disease; ns, not significant.

B cells and effector memory cluster of differentiation (CD) 8 T cells were highly correlated with the majority of the immune cells. Moreover, the correlation between the expression of the 6 signature genes and immune cells was examined and it was found that MTERF3 exhibited optimal correlation with macrophages, myeloid-derived suppressor cells (MDSC), regulatory T cell and activated CD8 T cells (Fig. 4C). It is noteworthy that MTERF3 exhibited the highest correlation with macrophages (Fig. 5).

MTERF3 expression is upregulated in CSE-treated 16HBE cells and MTERF3 deficiency suppresses the induction of apoptosis of 16HBE cells exposed to CSE. Based on the aforementioned results, the signature gene MTERF3 was experimentally validated in the following study. As shown in Fig. 6A, the viability of 16HBE cells was gradually decreased with the increase of CSE concentration compared with the control group. Immunoblotting revealed that CSE induction led to the upregulated MTERF3 expression; the highest MTERF3 expression level was observed in the CSE (4%) group (Fig. 6B). Therefore, CSE (4%) was selected for subsequent studies. It was shown (Fig. 6C) that MTERF3 expression was significantly downregulated in the siRNA-MTERF3-1 and siRNA-MTERF3-2 groups. 16HBE cells transfected with siRNA-MTERF3-1 were used to conduct subsequent experiments due to the lower MTERF3 expression. CCK-8 assay revealed that MTERF3 deficiency significantly elevated the viability of 16HBE cells treated by CSE compared with the CSE + siRNA-NC group (Fig. 6D). In addition, the apoptotic rate of 16HBE cells triggered by CSE was significantly decreased

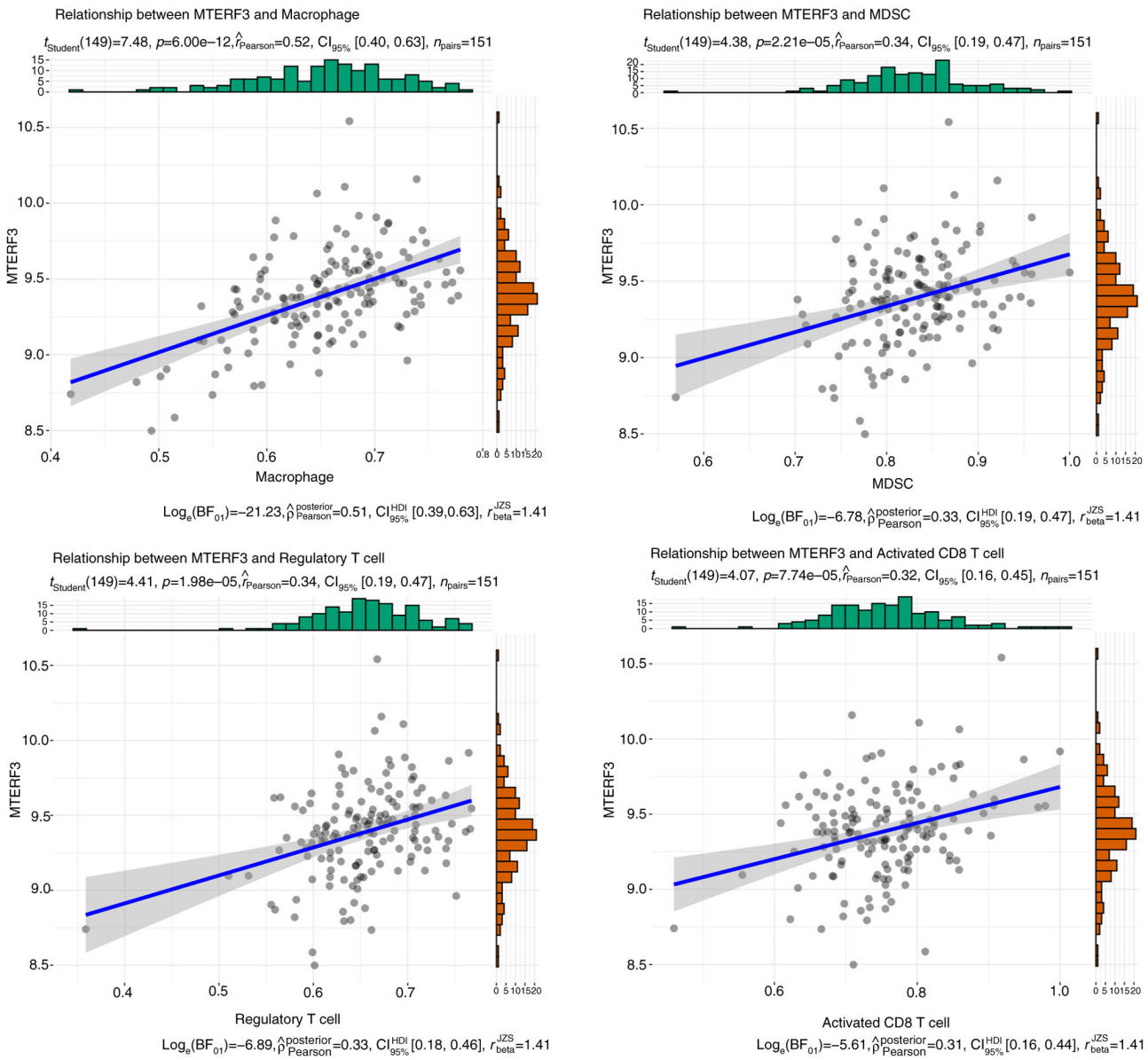

Figure 5. The correlation between MTERF3 and immune cells. The correlation between MTERF3 and macrophages, myeloid-derived suppressor cells, regulatory T cell and activated CD8 T cells. MTERF3, mitochondrial transcription termination factor 3; MDSC, myeloid-derived suppressor cells.

following knockdown of MTERF3 expression, as accompanied by the increased BCL2 expression and the decreased Bax and cleaved caspase 3 expressions (Fig. 6E and F).

Knockdown of MTERF3 expression promotes mitophagy in CSE-treated 16HBE cells. The effect of MTERF3 knockdown on mitophagy in CSE-treated 16HBE cells was explored in the following experiments. As shown in Fig. 7A and B, the increased MDA content and decreased SOD activity in the CSE group were significantly attenuated following MTERF3 loss-of-function in 16HBE cells. Of note, Mito SOX Red staining indicated that CSE-induced mitoROS accumulation in 16HBE cells was alleviated following siRNA-MTERF3 transfection (Fig. 7C). In addition, the decreased MMP expression caused by CSE in 16HBE cells was elevated following knockdown of MTERF3 expression (Fig. 7D). Moreover, CSE treatment prominently downregulated LC3II/LC3I, Beclin-1, PINK1 and Parkin (mitochondrion) expression levels, while it upregulated p62 and Parkin (cytoplasm) expression levels; this effect was reversed by MTERF3 depletion (Fig. 7E).

Discussion

As a heterogeneous lung disease, COPD is a global health burden (21). Based on publicly available databases, disease signature genes were screened for COPD. *In vitro* cell experiments were conducted using a CSE-induced bronchial epithelial cell model for validation and exploration. In the present study, 14 DEMRGs were identified. Following validation using the test dataset and LASSO regression, one DEMRG (MTERF3) was acquired. The *in vitro* cellular experiments further supported the regulation of MTERF3 on mitophagy.

Among them, autophagy exerts a crucial effect on the development and prognosis of COPD (22). Autophagy is a highly conserved homeostatic process, during which

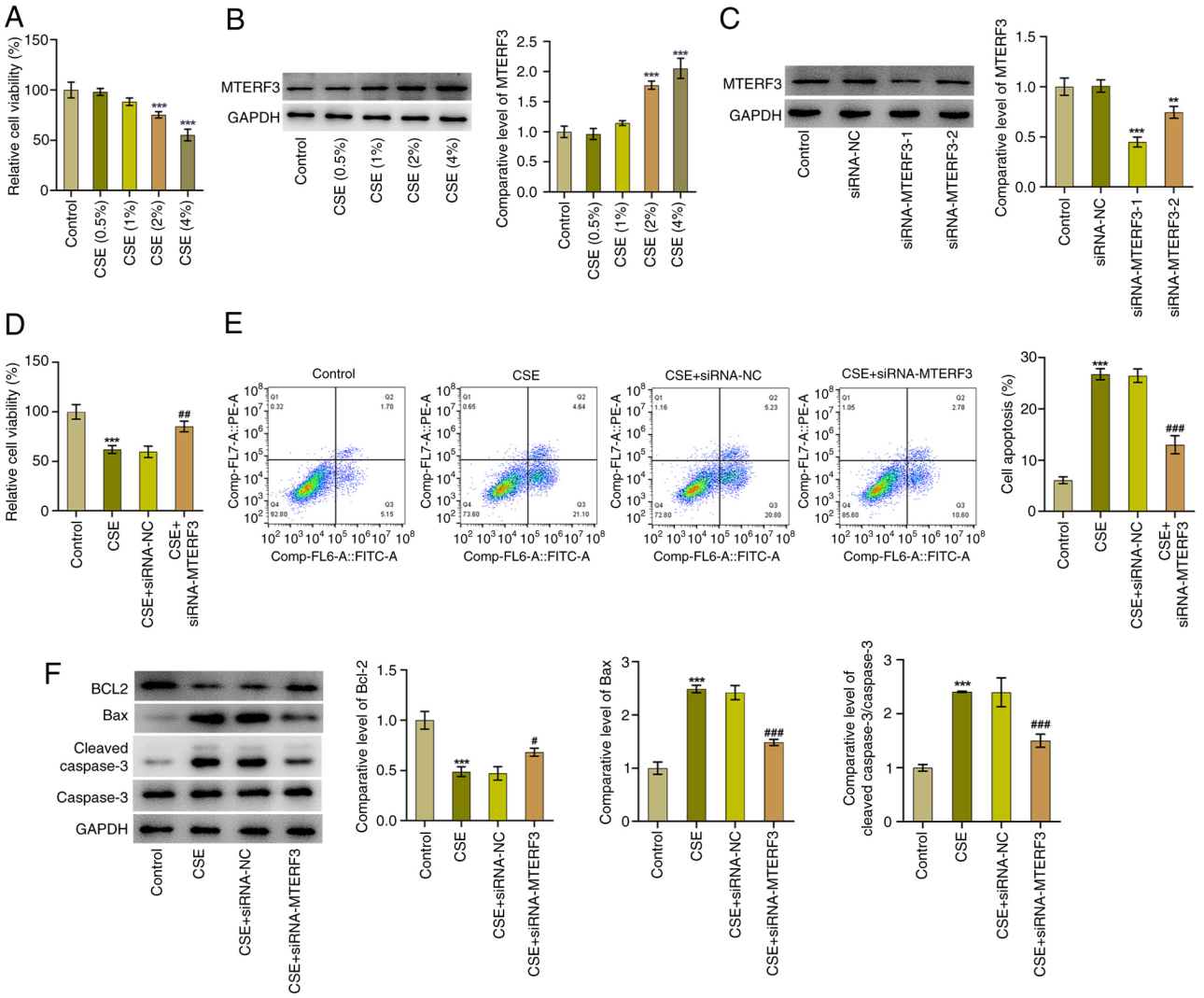

Figure 6. MTERF3 expression is upregulated in CSE-treated 16HBE cells and knockdown of its expression suppresses the induction of apoptosis of 16HBE cells exposed to CSE. (A) CCK-8 assay was used to detect 16HBE cell viability with or with CSE exposure. (B) Immunoblotting was employed to assess MTERF3 expression in 16HBE cells with or with CSE exposure. ***P<0.001 vs. control group. (C) Immunoblotting was used to assess MTERF3 expression in 16HBE cells following transfection. **P<0.01 and ***P<0.001 vs. siRNA-NC group. (D) The CCK-8 assay was used to detect the viability of MTERF3-silenced 16HBE cells exposed to CSE. (E) Flow cytometric analysis was used to detect the induction of apoptosis of MTERF3-silenced 16HBE cells exposed to CSE. (F) Immunoblotting was used to assess the expression of apoptosis-related proteins in MTERF3-silenced 16HBE cells exposed to CSE. ***P<0.001 vs. control group; #P<0.05, ##P<0.01 and ###P<0.001 vs. CSE + siRNA-NC group. MTERF3, mitochondrial transcription termination factor 3; CSE, cigarette smoke extract; CCK-8, Cell Counting Kit-8; cigarette smoke extract; siRNA, small interfering RNA; NC, negative control.

autophagosomes devour and degrade damaged or aged organelles for further processing and recycling to maintain cellular homeostasis (10). Notably, autophagy eliminates the damaged mitochondria, a process known as mitophagy, which is the main part of the mitochondrial quality control system (11). Dysregulation of mitophagy contributes to the development of diverse lung disorders, including asthma, acute lung injury, bronchopulmonary dysplasia and COPD (12).

A previous study has identified 40 potential autophagy-related genes of COPD through bioinformatics analysis, but no basic cell experiments were performed for verification (22). Mitophagy is the selective autophagy subtype specific for mitochondria, which exerts crucial effects on cell survival by maintaining energy homeostasis via its own catabolic activity (23,24). Impaired mitophagy, resulting in damaged or dysfunctional accumulation of mitochondria, has been demonstrated to be related to diverse pathological conditions; insufficient mitophagy participates in the pathogenesis of COPD (14,25). By enhancing mitophagy, Bufei Yishen formula III attenuates COPD rat pulmonary dysfunction and CSE-induced airway epithelial cell damage (26). PINK1 and Parkin, two key markers related to mitophagy, exhibit downregulated expression levels in lung tissues of COPD mice exposed to CSE (27). Recently, Wang *et al* (28) demonstrated that pre-treatment with a mitophagy activator alleviated CSE-induced oxidative stress, improved mitochondrial dysfunction, downregulated p62 levels and elevated LC3B-II/I ratio in alveolar and airway epithelial cells. In the present study, CSE treatment impaired mitophagy in human bronchial epithelial cells, as demonstrated by downregulation of LC3II/LC3I, Beclin-1, PINK1 and Parkin (mitochondrion) expressions, upregulation of p62 and Parkin (cytoplasm) expressions as well as enhanced MitoSOX fluorescence intensity and reduced MMP levels.

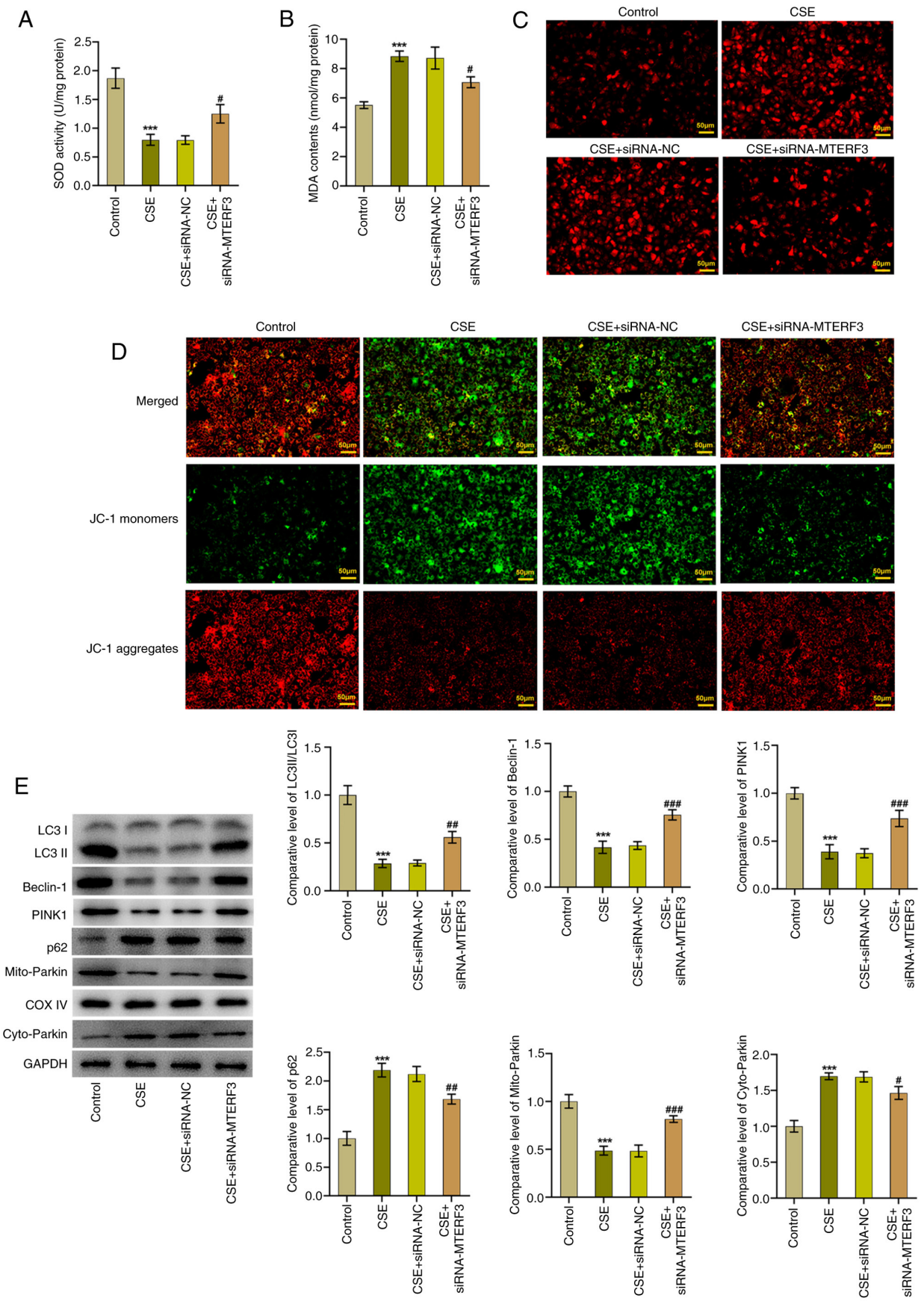

Figure 7. Knockdown of MTERF3 expression promotes mitophagy in CSE-treated 16HBE cells. (A) MDA content and (B) SOD activity were detected using the corresponding kits. (C) The generation of mitoROS was assessed with the application of Mito SOX Red staining. (D) MMP was evaluated using JC-1 staining. (E) Immunoblotting was employed to assess the expression of mitophagy-related proteins. ***P<0.001 vs. control group; $^{\#}$P<0.05, $^{\#\#}$P<0.01 and $^{\#\#\#}$P<0.001 vs. CSE + siRNA-NC group. MTERF3, mitochondrial transcription termination factor 3; CSE, cigarette smoke extract; MDA, malondialdehyde; SOD, superoxide dismutase; MMP, matrix metalloproteinase; JC-1, 5,5',6,6'-tetrachlorol,1',3,3'-tetramethylbenzimidazolylcarbocyanine iodide; siRNA, small interfering RNA; NC, negative control.

In the present study, MTERF3 displayed significant variability in expression in both the training and validation sets, demonstrating high specificity and diagnostic performance. MTERF3 is the most highly conserved member of the MTERF protein family (29). As reported, MTERF3 functions as a negative regulator of mitochondrial DNA transcription (30). Accumulating research has confirmed that MTERF3 is implicated in diseases associated with mitochondrial dysfunction (31,32). A recent study on Parkinson's disease has shown that MTERF3 facilitates 1-methyl-4-phenylpyridinium ion-induced mitochondrial dysfunction in SH-SY5Y cells (33). In addition, MTERF3 expression is upregulated in lung adenocarcinoma and interference with MTERF3 obviously restrains the proliferation and migration of lung cancer cells while contributing to mitophagy and the production of MitoSOX (34). The present study was the first to explore the expression and role of MTERF3 in CSE-treated 16HBE cells. The results demonstrated that MTERF3 expression was elevated in CSE-treated 16HBE cells and MTERF3 depletion suppressed the induction of apoptosis and promoted mitophagy in CSE-treated 16HBE cells.

Accumulating evidence has shown that immune cells are linked to the development of COPD (35,36). Significantly higher type 1 T helper cells but lower levels of type 2 T helper cells have been found in the peripheral blood from patients with COPD (37). A previous study has also reported the elevated alveolar macrophage alveolar space in patients with COPD (38). A negative association has been shown between the number of neutrophils and the degree of alveolar destruction in smokers, in contrast to alveolar macrophages (39). As reported, the percentage of natural killer cells notably decreased in patients with COPD compared with healthy non-smokers (40). The increases in B cell counts lung tissues of patients with COPD is correlated directly with COPD severity (41). In patients with COPD, long-term CS increases regulatory T cells in the airways (42). Specifically, Sales *et al* (43) demonstrated that the role of regulatory T cells in regulating immune response may vary in different lung regions of patients with COPD. Emerging evidence has supported the notion that CD8 T cells are notably increased in lung tissues of patients with mild-moderate COPD (38). Consistent with the aforementioned studies, the current study revealed that the infiltrating abundance of the majority of immune cells, such as activated CD8 T cells, regulatory T cells and activated B cells, was higher in COPD samples than that noted in control samples. Additionally, significantly reduced proportion of natural killer cells and neutrophils were found in in COPD samples. These results suggested that these immune cells were potentially associated with the pathogenesis of COPD. Moreover, it was found that MTERF3 exhibited optimal correlation with macrophages, MDSCs, regulatory T cells and activated CD8 T cells. The present study suggested that MTERF3 exhibited optimal correlation with multiple immune cells. The exact role of immune cells and MTERF3 requires further investigations using basic research experiments in the future.

However, certain limitations should be noted in the current study. First of all, the bioinformatics results were acquired from lung tissues of patients with COPD. Nevertheless, the verification was conducted in small airway epithelium of included individuals. Secondly, there was no information about the inclusion and exclusion criteria used in selecting the COPD and control samples on GEO datasets. Additionally, the exact role of immune cells and their association with signature genes require further investigations using basic research experiments. Lastly, the inclusion of additional validation cohorts is crucial to ensure the sensitivity and reliability of the diagnostic performance noted in the present study.

In summary, the present study identified a key signature gene (MTERF3) related to mitophagy in COPD via bioinformatic analysis. *In vitro* experiments demonstrated that MTERF3 expression was upregulated in CSE-treated bronchial epithelial cells and that MTERF3 deficiency promoted mitophagy. These findings expand our understanding on COPD and offer novel perspectives for the diagnosis and treatment of this condition.

Acknowledgements

Not applicable.

Funding

No funding was received.

Availability of data and materials

The data generated in the present study may be requested from the corresponding author.

Authors' contributions

JC and GS contributed to the conception and design of this study. JC and XZ analyzed the data and drafted the manuscript. GS contributed to make the figures and revised the manuscript. JC, GS and XZ participated in the experiments. All authors read and approved the final version of the manuscript. JC and GS confirm the authenticity of all the raw data.

Ethics approval and consent to participate

Not applicable.

Patient consent for publication

Not applicable.

Competing interests

The authors declare that they have no competing interests.

References

1. López-Campos JL, Tan W and Soriano JB: Global burden of COPD. Respirology 21: 14-23, 2016.
2. Safiri S, Carson-Chahhoud K, Noori M, Nejadghaderi SA, Sullman MJM, Ahmadian Heris J, Ansarin K, Mansournia MA, Collins GS, Kolahi AA and Kaufman JS: Burden of chronic obstructive pulmonary disease and its attributable risk factors in 204 countries and territories, 1990-2019: Results from the Global Burden of Disease Study 2019. BMJ 378: e069679, 2022.

3. Boers E, Barrett M, Su JG, Benjafield AV, Sinha S, Kaye L, Zar HJ, Vuong V, Tellez D, Gondalia R, *et al*: Global burden of chronic obstructive pulmonary disease through 2050. JAMA Netw Open 6: e2346598, 2023.
4. Hikichi M, Mizumura K, Maruoka S and Gon Y: Pathogenesis of chronic obstructive pulmonary disease (COPD) induced by cigarette smoke. J Thorac Dis 11 (Suppl 17): S2129-S2140, 2019.
5. GBD 2019 Diseases and Injuries Collaborators: Global burden of 369 diseases and injuries in 204 countries and territories, 1990-2019: A systematic analysis for the Global burden of disease study 2019. Lancet 396: 1204-1222, 2020.
6. Mei J, Zhang Y, Lu S and Wang J: Long non-coding RNA NNT-AS1 regulates proliferation, apoptosis, inflammation and airway remodeling of chronic obstructive pulmonary disease via targeting miR-582-5p/FBXO11 axis. Biomed Pharmacother 129: 110326, 2020.
7. Lee KY, Ho SC, Sun WL, Feng PH, Lin CW, Chen KY, Chuang HC, Tseng CH, Chen TT and Wu SM: Lnc-IL7R alleviates PM(2.5)-mediated cellular senescence and apoptosis through EZH2 recruitment in chronic obstructive pulmonary disease. Cell Biol Toxicol 38: 1097-1120, 2022.
8. Barnes PJ, Baker J and Donnelly LE: Autophagy in asthma and chronic obstructive pulmonary disease. Clin Sci (Lond) 136: 733-746, 2022.
9. Lv X, Li K and Hu Z: Chronic obstructive pulmonary disease and autophagy. Adv Exp Med Biol 1207: 559-567, 2020.
10. Mizushima N and Komatsu M: Autophagy: Renovation of cells and tissues. Cell 147: 728-741, 2011.
11. Lu Y, Li Z, Zhang S, Zhang T, Liu Y and Zhang L: Cellular mitophagy: Mechanism, roles in diseases and small molecule pharmacological regulation. Theranostics 13: 736-766, 2023.
12. Sharma A, Ahmad S, Ahmad T, Ali S and Syed MA: Mitochondrial dynamics and mitophagy in lung disorders. Life Sci 284: 119876, 2021.
13. Ito S, Araya J, Kurita Y, Kobayashi K, Takasaka N, Yoshida M, Hara H, Minagawa S, Wakui H, Fujii S, *et al*: PARK2-mediated mitophagy is involved in regulation of HBEC senescence in COPD pathogenesis. Autophagy 11: 547-559, 2015.
14. Ahmad T, Sundar IK, Lerner CA, Gerloff J, Tormos AM, Yao H and Rahman I: Impaired mitophagy leads to cigarette smoke stress-induced cellular senescence: Implications for chronic obstructive pulmonary disease. FASEB J 29: 2912-2929, 2015.
15. Zhang M, Fang L, Zhou L, Molino A, Valentino MR, Yang S, Zhang J, Li Y and Roth M: MAPK15-ULK1 signaling regulates mitophagy of airway epithelial cell in chronic obstructive pulmonary disease. Free Radic Biol Med 172: 541-549, 2021.
16. Zhang MY, Jiang YX, Yang YC, Liu JY, Huo C, Ji XL and Qu YQ: Cigarette smoke extract induces pyroptosis in human bronchial epithelial cells through the ROS/NLRP3/caspase-1 pathway. Life Sci 269: 119090, 2021.
17. Liu YB, Hong JR, Jiang N, Jin L, Zhong WJ, Zhang CY, Yang HH, Duan JX and Zhou Y: The role of mitochondrial quality control in chronic obstructive pulmonary disease. Lab Invest 104: 100307, 2024.
18. Tulen CBM, Wang Y, Beentjes D, Jessen PJJ, Ninaber DK, Reynaert NL, van Schooten FJ, Opperhuizen A, Hiemstra PS and Remels AHV: Dysregulated mitochondrial metabolism upon cigarette smoke exposure in various human bronchial epithelial cell models. Dis Model Mech 15: dmm049247, 2022.
19. Trivedi A, Khan MA, Bade G and Talwar A: Orchestration of neutrophil extracellular traps (Nets), a unique innate immune function during chronic obstructive pulmonary disease (COPD) development. Biomedicines 9: 53, 2021.
20. Schivo M, Albertson TE, Haczku A, Kenyon NJ, Zeki AA, Kuhn BT, Louie S and Avdalovic MV: Paradigms in chronic obstructive pulmonary disease: Phenotypes, immunobiology, and therapy with a focus on vascular disease. J Investig Med 65: 953-963, 2017.
21. Mathioudakis AG, Janssens W, Sivapalan P, Singanayagam A, Dransfield MT, Jensen JS and Vestbo J: Acute exacerbations of chronic obstructive pulmonary disease: In search of diagnostic biomarkers and treatable traits. Thorax 75: 520-527, 2020.
22. Sun S, Shen Y, Wang J, Li J, Cao J and Zhang J: Identification and validation of autophagy-related genes in chronic obstructive pulmonary disease. Int J Chron Obstruct Pulmon Dis 16: 67-78, 2021.
23. Ni HM, Williams JA and Ding WX: Mitochondrial dynamics and mitochondrial quality control. Redox Biol 4: 6-13, 2015.
24. Palikaras K, Lionaki E and Tavernarakis N: Mechanisms of mitophagy in cellular homeostasis, physiology and pathology. Nat Cell Biol 20: 1013-1022, 2018.
25. Wang S, Long H, Hou L, Feng B, Ma Z, Wu Y, Zeng Y, Cai J, Zhang DW and Zhao G: The mitophagy pathway and its implications in human diseases. Signal Transduct Target Ther 8: 304, 2023.
26. Li MY, Qin YQ, Tian YG, Li KC, Oliver BG, Liu XF, Zhao P and Li JS: Effective-component compatibility of Bufei Yishen formula III ameliorated COPD by improving airway epithelial cell senescence by promoting mitophagy via the NRF2/PINK1 pathway. BMC Pulm Med 22: 434, 2022.
27. Wang Q, Unwalla H and Rahman I: Dysregulation of mitochondrial complexes and dynamics by chronic cigarette smoke exposure Utilizing MitoQC reporter mice. Mitochondrion 63: 43-50, 2022.
28. Wang S, Song X, Wei L, Liu Q, Li C and Wang J: Role of mitophagy in cigarette smoke-induced lung epithelial cell injury in vitro. Curr Mol Med 23: 1130-1140, 2023.
29. Roberti M, Polosa PL, Bruni F, Deceglie S, Gadaleta MN and Cantatore P: MTERF factors: A multifunction protein family. Biomol Concepts 1: 215-224, 2010.
30. Park CB, Asin-Cayuela J, Cámara Y, Shi Y, Pellegrini M, Gaspari M, Wibom R, Hultenby K, Erdjument-Bromage H, Tempst P, *et al*: MTERF3 is a negative regulator of mammalian mtDNA transcription. Cell 130: 273-285, 2007.
31. Zheng Z, Zhao Y, Yu H, Wang T, Li J, Xu L, Ding C, He L, Wu L and Dong Z: Suppressing MTERF3 inhibits proliferation of human hepatocellular carcinoma via ROS-mediated p38 MAPK activation. Commun Biol 7: 18, 2024.
32. Andersson DC, Fauconnier J, Park CB, Zhang SJ, Thireau J, Ivarsson N, Larsson NG and Westerblad H: Enhanced cardiomyocyte Ca(2+) cycling precedes terminal AV-block in mitochondrial cardiomyopathy Mterf3 KO mice. Antioxid Redox Signal 15: 2455-2464, 2011.
33. Zhu S, Xu N, Han Y, Ye X, Yang L, Zuo J and Liu W: MTERF3 contributes to MPP+-induced mitochondrial dysfunction in SH-SY5Y cells. Acta Biochim Biophys Sin (Shanghai) 54: 1113-1121, 2022.
34. Wang J, Liu K, Li J, Zhang H, Gong X, Song X, Wei M, Hu Y and Li J: Constructing and evaluating a mitophagy-related gene prognostic model: Implications for immune landscape and tumor biology in lung adenocarcinoma. Biomolecules 14: 228, 2024.
35. Ma R, Su H, Jiao K and Liu J: Role of Th17 cells, Treg cells, and Th17/Treg imbalance in immune homeostasis disorders in patients with chronic obstructive pulmonary disease. Immun Inflamm Dis 11: e784, 2023.
36. Kim RY and Oliver B: Innate immune reprogramming in chronic obstructive pulmonary disease: New mechanisms for old questions. Am J Respir Cell Mol Biol 68: 470-471, 2023.
37. Chen G, Mu Q and Meng ZJ: Cigarette smoking contributes to Th1/Th2 cell dysfunction via the cytokine milieu in chronic obstructive pulmonary disease. Int J Chron Obstruct Pulmon Dis 18: 2027-2038, 2023.
38. Villaseñor-Altamirano AB, Jain D, Jeong Y, Menon JA, Kamiya M, Haider H, Manandhar R, Sheikh MDA, Athar H, Merriam LT, *et al*: Activation of CD8(+) T cells in chronic obstructive pulmonary disease lung. Am J Respir Crit Care Med 208: 1177-1195, 2023.
39. Kotlyarov S: Involvement of the innate immune system in the pathogenesis of chronic obstructive pulmonary disease. Int J Mol Sci 23: 985, 2022.
40. Urbanowicz RA, Lamb JR, Todd I, Corne JM and Fairclough LC: Altered effector function of peripheral cytotoxic cells in COPD. Respir Res 10: 53, 2009.
41. Polverino F, Seys LJ, Bracke KR and Owen CA: B cells in chronic obstructive pulmonary disease: moving to center stage. Am J Physiol Lung Cell Mol Physiol 311: L687-l695, 2016.
42. Smyth LJ, Starkey C, Vestbo J and Singh D: CD4-regulatory cells in COPD patients. Chest 132: 156-163, 2007.
43. Sales DS, Ito JT, Zanchetta IA, Annoni R, Aun MV, Ferraz LFS, Cervilha DAB, Negri E, Mauad T, Martins MA and Lopes FDTQS: Regulatory T-Cell distribution within lung compartments in COPD. COPD 14: 533-542, 2017.